

Parametric Mapping of 5HT_{1A} Receptor Sites in the Human Brain with the Hypotime Method: Theory and Normal Values

Mette Møller, Anders Rodell, and Albert Gjedde

Center of Functionally Integrative Neuroscience, Aarhus University, and Pathophysiology and Experimental Tomography Center, Aarhus University Hospitals, Aarhus, Denmark

The radioligand [carbonyl-¹¹C]WAY-100635 (¹¹C-WAY) is a PET tracer of the serotonin 5HT_{1A} receptors in the human brain. It is metabolized so rapidly in the circulation that it behaves more as a chemical microsphere than as a tracer subject to continuous exchange between the circulation and brain tissue. Although reference tissue methods are useful as analyses of uptake of some radioligands with indeterminate arterial input functions, their use to analyze ¹¹C-WAY uptake and binding is challenged by the rapid plasma metabolism, which violates the assumption that regions of interest and reference regions continue to exchange radioligand with the circulation during the entire uptake period. Here, we proposed a method of calculation (Hypotime) that specifically uses the washout rather than the accumulation of ¹¹C-WAY to determine binding potentials (BP_{ND}), without the use of regression analysis. **Methods:** A total of 19 healthy volunteers (age range, 23–73 y) underwent PET to test the Hypotime application of the chemical microsphere properties of ¹¹C-WAY to identify regions of binding and nonbinding on the exclusive basis of the rate of washout of ¹¹C-WAY. **Results:** The results of the Hypotime method were compared with the simplified but multilinearized reference tissue method (MLSRTM). The distribution of receptor BP_{ND} obtained with Hypotime was consistent with previous autoradiography of postmortem brain tissue, with the highest values of BP_{ND} recorded in the medial temporal lobe and decline of receptor availability with age. The values in the basal ganglia and cerebellum were negligible. The MLSRTM, in contrast, yielded lower BP_{ND} in all regions and only weakly revealed the decline with age. **Conclusion:** The simple and computationally efficient Hypotime method gave reliable values of BP_{ND} without the use of regression. The MLSRTM, on the other hand, appeared to be affected by the early disappearance of the radioligand from the circulation and the associated uncertain late presence of ¹¹C-WAY in the circulation.

Key Words: neurotransmission; serotonin 5HT_{1A} receptors; PET; ¹¹C-WAY-100635; Hypotime

J Nucl Med 2009; 50:1229–1236

DOI: 10.2967/jnumed.108.053322

The radioligand [carbonyl-¹¹C]WAY-100635 (¹¹C-WAY) binds to the serotonin 5HT_{1A} receptor as an antagonist. The ligand has been used to map the neuroreceptors in healthy subjects and in patients with diseases as diverse as major depression (1), bulimia nervosa (2), amyotrophic lateral sclerosis (3), schizophrenia (4), Parkinson disease (5), and temporal lobe epilepsy (6). In general, intrasubject variability of the binding is low, but intersubject variability is high (7,8). Although the receptor binding potentials (BP_{ND}) globally decline in depression, other diseases reveal only subtle changes, and demographic, physiologic, and psychologic measures do not consistently explain the highly variable receptor availability reported for healthy subjects. We recently reported a 3% reduction of the availability of the BP_{ND} of this receptor per decade of life in healthy volunteers (9), but the evidence for an age-related decline is still subject to uncertainty because of the wide variability of the results (7,10,11).

Studies in both humans and animals generally reveal that the BP_{ND} is insensitive to changes of the concentration of endogenous serotonin in brain tissue (1,12–14). These variable findings raise the question of whether the diversity of BP_{ND} values among people measured with ¹¹C-WAY reflects a true heterogeneity of the density of 5HT_{1A} receptors or whether methodologic issues concerning the correct quantification of the BP_{ND} could contribute to the variability.

Three problems complicate the correct quantification of 5HT_{1A} receptor binding with ¹¹C-WAY. The first of the 3 potential biases is the rapid metabolism of the tracer in the circulation (15,16). The rapid disappearance of the tracer from the circulation and the consequent brief exchange with brain tissue imply that the tracer could behave much like a chemical microsphere. Conventional tracer uptake normally occurs over a period of time as a continuous function of the magnitude of the arterial input function, whereas with microspheres, the actual arterial input function is difficult to determine because its temporal extent is limited to that of a narrow spike.

In receptor mapping, the reference tissue method is popular because it appears to eliminate the need to measure

Received Apr. 9, 2008; revision accepted Apr. 9, 2009.

For correspondence or reprints contact: Mette Møller, PET Center, Aarhus University Hospital, Nørrebrogade 44, 8000 Aarhus C, Denmark.

E-mail: moller@pet.auh.dk

COPYRIGHT © 2009 by the Society of Nuclear Medicine, Inc.

the arterial input function of a tracer, particularly in the cases of tracers that behave as chemical microspheres. However, as in the case of ^{11}C -WAY, the rapid metabolism in turn may violate the fundamental assumption that both the reference region and the pool of free tracer in the binding regions continue to exchange significant quantities of tracer with the circulation. In the absence of a continuing source of tracer in the circulation, reference and binding regions independently clear tracer from the respective volumes of distribution, and tracer in the reference region no longer is a proper surrogate for tracer in the circulation. The time–activity functions of different regions now depend on regional properties of binding, blood flow, and blood–brain barrier permeability, rather than on a common source of tracer in the circulation.

The second potential problem is the uncertainty about a proper region of reference. The adult cerebellum is believed to be almost devoid of 5HT_{1A} receptors (17). Although they may be present in this part of the brain in fetal and early life, the density declines with age. Recent studies of the adult brain (8,18) demonstrate specific residual binding in vermis and cortex of cerebellum that may lead to the underestimation of binding in other regions if vermis and cortex of cerebellum are included in the reference region. In 3 studies with ^{11}C -WAY (3,5,7), as many as 10% of the subjects were excluded because of abnormally high cerebellar time–activity curves. The underlying causes were not examined, but specific binding in the cerebellum or incorrect segmentation of the cerebellum are plausible explanations.

The third potential problem is the influence of blood flow and blood–brain barrier permeability differences in regions of specific binding. If the tracer is subject to clearance from multiple compartments having pools of exchangeable tracer and of tracer bound to receptors, it is possible that both flow and permeability changes can mimic or mask changes of binding.

In the present study, to establish a method of global parametric mapping of the BP_{ND} of ^{11}C -WAY that takes the particular kinetic properties of ^{11}C -WAY into account, we compared 2 methods of noninvasive assay of ^{11}C -WAY binding in the brain of healthy subjects. First, we applied a model of tracer clearance, Hypotime, which we designed to map the washout of the tracer from specifically and non-specifically binding regions. Measures of regional tracer clearances were used to identify a reference region of negligible specific binding. The reference region subsequently was used to obtain parametric maps of BP_{ND} by means of a second method, a multilinearized simplified reference tissue method (MLSRTM), expressed as Equation 9 in a recent application of the method (19). In this method, the BP_{ND} values are estimated by conventional weighted multilinear regression of operational equations of integral form to the same regional records and as such depend on a common source of tracer in the circulation for the duration of data acquisition.

MATERIALS AND METHODS

The Research Ethics Committee of Aarhus County approved the recruitment of 19 healthy volunteers (age range, 23–73 y; 8 women, 11 men) into 2 groups, with an average age in the group of 12 elderly subjects of 62.5 ± 6.8 y (mean \pm SD) and an average age in the group of 7 young subjects of 25.1 ± 2.0 y. All volunteers gave written informed consent to participate in the study. Exclusion criteria included cardiovascular disease and any history of neurologic and psychiatric disease. All subjects were physically fit, were free of prescribed medication, and did not meet the criteria for depression according to the *Diagnostic and Statistical Manual of Mental Disorders* (20).

Radiochemistry

The radioligand ^{11}C -WAY was synthesized from the cyclotron-generated precursor according to the method of McCarron et al. (21). In brief, ^{11}C was collected in a stainless steel cryotrap, warmed, and then flushed with nitrogen through a small coil of 0.2-cm-outer-diameter polypropylene tubing, which had been earlier flushed with a solution of cyclohexylmagnesium chloride (500 μL of 0.5 M in tetrahydrofuran). The ^{11}C -labeled Grignard adduct, ^{11}C -cyclohexanecarbonyl chloride, was eluted with a solution of thionyl chloride (10 μL in 400 μL THF) into a septum-sealed vial (2 mL) containing WAY-100634 (2 mg), 50- μL THF, and triethylamine (60 μL) under a nitrogen atmosphere. The reaction proceeded in 7 min at 85°C. The crude product was diluted with 500 μL of high-performance liquid chromatography (HPLC) eluent, and purified by reversed-phase HPLC on a Ultracarb 7 ODS 30 column (250 \times 10 mm; Phenomenex Ltd.), eluting with sterile ethanol:70 mM NaH_2PO_4 (52:48) at 6 mL/min. The fraction containing ^{11}C -WAY-100635 (retention time, \sim 10 min) was collected, evaporated to near-dryness at 90°C under vacuum, and then reformulated in sterile saline (10 mL) before it was passed through a sterile 0.22- μm filter into a sterile vial. Injected masses were 31 nmol (SEM, 5.8 nmol) and 12 nmol (SEM, 2.5 nmol) in the groups of young and elderly subjects, respectively. Specific radioactivities were 36 GBq/ μmol (SEM, 7.9) in the group of young subjects and 38 GBq/ μmol (SEM, 7.8) in the group of elderly subjects.

PET

Subjects were positioned in the ECAT EXACT HR47 tomograph (CTI/Siemens). After a 15-min attenuation, a single-frame scan was acquired, starting at 60,000 true counts per second after an intravenous bolus injection of ^{15}O - H_2O (500 MBq), followed by bolus injection of ^{11}C -WAY (150–430 MBq; mean, 270 MBq; SD, 111 MBq) and the initiation of 60-min emission recordings of 22 frames in 3-dimensional mode. High-resolution T1-weighted MR images were obtained at 1.5 or 3 T (GE Sigma Systems). The summed emission recordings were automatically coregistered to the individual MRI scans using 6 parameters. Individual MR images were coregistered to a common stereotactic space (Montreal Neurologic Institute) (22) using a 12-parameter affine rigid-body transformation; registrations were automatic in the young group but manual in the elderly group because of the inadequate registration of atrophied brains. After the calculation of the final PET-Talairach transformation matrix, dynamic emission recordings were resampled into common coordinates.

We used the program Display (<http://www.bic.mni.mcgill.ca/software/distribution>) to draw templates of regions of interest (ROIs) bilaterally on the average MR images, identifying the hippocampus and the insular, cingulate, and ventral medial prefrontal

cortices. Because of central and cortical atrophy in the elderly subjects, each of the 8 regions was adjusted to the individual resampled MR images. The raphé nuclei were not visible on MR images and were outlined on the individual images in each subject.

Data Analyses

Hypotime Method. In the case of negligible input from the circulation, the tissue time–activity curves of the radioligand are dominated by washout from the brain regions of uptake. The method specifically developed to take this condition into account, Hypotime, is based only on the differences among washout rates from regions with different properties of binding, blood flow rates, and blood–brain barrier permeability. To determine the rates of washout from regions of binding and a reference region of no specific binding, the following linked differential equations were solved, assuming homogeneity of single voxels. The first equation gives the rate of decay of tracer in a voxel of binding,

$$\frac{dm_{[2_1+3_1]}^*}{dt} = -k'_{2_1} m_{[2_1+3_1]}^*, \quad \text{Eq. 1}$$

where $m_{[2_1+3_1]}^*$ is the total quantity of tracer radioligand in non-binding (subscript 2) and binding (subscript 3) compartments of a voxel having specific binding (subsubscript 1) of the tracer radioligand (23). As the fractional clearance or washout rate from the radioligand compartments in a region of specific binding, the rate constant k'_{2_1} for an apparent first-order decay is defined as,

$$k'_{2_1} = \frac{k_{2_1}k_{4_1}}{k_{3_1} + k_{4_1}} = \frac{k_{2_1}}{1 + BP_{ND}}, \quad \text{Eq. 2}$$

provided the rates of association and dissociation are sufficiently rapid, as assumed for the 1-compartment first-order kinetics where k_{2_1} is the rate of removal across the blood–brain barrier, and BP_{ND} is the binding potential relative to nondisplaceable tracer, equal to the ratio k_{3_1}/k_{4_1} . The rate constants k_{3_1} and k_{4_1} are the constants of association and dissociation, respectively. For a voxel with a single extravascular tracer accumulation compartment (subscript 2) in a region of no specific binding (subsubscript 2), Equation 1 reduces to,

$$\frac{dm_{2_2}^*}{dt} = -k_{2_2} m_{2_2}^*, \quad \text{Eq. 3}$$

where k_{2_2} is the fractional clearance or washout rate of the tracer from such a reference voxel of no binding, and $m_{2_2}^*$ is the quantity of tracer in such a reference voxel. The solutions to each of these differential equations predict the monoexponential washout of the radioligand from the respective voxels. When T is the time of the last frame of the positron emission tomograms, the ratio between the twice-integrated and the once-integrated solutions to Equations 1 and 3 is the Hypotime measure, which has a unit of time but a magnitude less than real time (hence the term *Hypotime*). The value depends on the magnitudes of the decay constants k'_{2_1} and k_{2_2} as follows,

$$\Theta'' = \frac{\int_0^T \int_0^u m_{2_1}^* dt du}{\int_0^T m_{2_1}^* dt} = \frac{T}{1 - e^{-k'_{2_1}T}} - \frac{1}{k'_{2_1}}, \quad \text{Eq. 4}$$

where Θ is the Hypotime measure. The maximum value that Θ'' can attain is T, consistent with an infinitely high washout rate, and the minimum is T/2, consistent with absent washout and

permanent deposit of the radioactivity in the tissue, in which case the chemical microsphere is now stuck permanently in the tissue and the BP_{ND} is infinitely high. The magnitude of this measure in voxels of no binding defines the reference value (Θ''_{ref}) as,

$$\Theta''_{ref} = \frac{\int_0^T \int_0^u m_{2_2}^* dt du}{\int_0^T m_{2_2}^* dt} = \frac{T}{1 - e^{-k_{2_2}T}} - \frac{1}{k_{2_2}}, \quad \text{Eq. 5}$$

where the rate constant k_{2_2} is the relaxation constant of the reference region. The rate constant k_{2_2} incorporates the combined effects of blood flow, the physical distribution volume of the tracer (equal to the partition coefficient in the absence of specific binding), and the permeability of the blood–brain barrier to the tracer. These properties are expressed in the unidirectional clearance of the tracer. Equations 4 and 5 are not easily solved for k'_{2_1} or k_{2_2} , but a solution is provided by the growth equation of Gompertz (24),

$$\Theta'' = T e^{\ln(1/2)e^{-k_{2_2}/\alpha}}, \quad \text{Eq. 6}$$

which, when expressed with the notation used here, yields the solutions,

$$k'_{2_1} = -\alpha \ln \left[\frac{\ln \frac{\Theta''}{T}}{\ln \frac{1}{2}} \right] \quad \text{and} \quad k_{2_2} = -\alpha \ln \left[\frac{\ln \frac{\Theta''_{ref}}{T}}{\ln \frac{1}{2}} \right], \quad \text{Eq. 7}$$

where α is a scaling factor characteristic of the duration of integration, which is eliminated by the use of ratios. The clearance from a voxel in a binding region relative to the clearance observed in the reference region defines the clearance ratio R_1 , equal to the ratio K_{1_1}/K_{1_2} , where K_{1_2} is the clearance from a nonbinding voxel in the reference region,

$$R_1 = \frac{K_{1_1}}{K_{1_2}} = \frac{k_{2_1}}{k_{2_2}}, \quad \text{Eq. 8}$$

where R_1 is the ratio between the voxel values at the time of the peak accumulation of radioactivity, relative to the reference region, when other terms have the meaning described above. The decay of the time–activity curves is thus given by the solution to Equations 2 and 8,

$$k'_{2_1} = \frac{k_{2_1}k_{4_1}}{k_{3_1} + k_{4_1}} = \frac{k_{2_1}}{1 + p_B} = \frac{R_1 k_{2_2}}{1 + BP_{ND}}, \quad \text{Eq. 9}$$

where the symbols have the same meaning as above. The solution to Equation 9 is,

$$BP_{ND} = R_1 \left(\frac{k_{2_2}}{k'_{2_1}} \right) - 1, \quad \text{Eq. 10}$$

which yields the operational equation of the BP_{ND} when the expressions given in Equation 7 are inserted into Equation 10,

$$BP_{ND} = R_1 \left(\frac{\ln \left(\frac{\ln \left(\frac{\Theta''_{ref}}{T} \right) / \left[\ln \frac{1}{2} \right]}{\ln \left(\frac{\Theta''}{T} \right) / \left[\ln \frac{1}{2} \right]} \right)}{\ln \left(\frac{\Theta''_{ref}}{T} \right) / \left[\ln \frac{1}{2} \right]} \right) - 1, \quad \text{Eq. 11}$$

which has a simpler solution when $k_2 \leq 0.05$,

$$BP_{ND} = R_1 \left(\frac{\Theta''_{ref} - \frac{T}{2}}{\Theta'' - \frac{T}{2}} \right) - 1. \quad \text{Eq. 12}$$

MLSRTM

The MLSRTM expressed in Equation 9 in the study by Zhou et al. (19) estimates the BP_{ND} by conventional weighted multilinear regression of operational equations of integral form to the regional records identified above. In the application of the method, we used the authors' Equation 9 without the spatial constraint added in that article to smooth regional values to a regional average.

Common Reference Region Mask

Washout from an ROI can be slow because the flow rate is low or because the distribution volume is high, or both. From the reference tissue we require a relationship between the rate of washout and the initial clearance (as a measure of blood flow) in a tissue that has the least binding possible. Thus 2 requirements must be fulfilled of the reference, that is, that the tissue has no specific binding and that the composition of the tissue is homogeneous to provide the most precise relationship between the initial tracer clearance to the reference tissue and the Hypotime variable in the reference tissue.

The calculated Θ'' values of all voxels were used to segment the tissue into groups on the basis of major subdivisions of values and hence were used to specify the region of presumed absence of specific binding. The Θ'' map confirmed the suspected heterogeneity of cerebellar uptake, with the lowest Θ'' values in cortex and vermis and the highest washout rates in white matter. The mask was delineated to match the white matter of the cerebellum.

RESULTS

Reference Region Mask

Voxel maps of the Hypotime measure Θ'' , calculated according to Equation 4, identified a region of no specific binding of the radioligand in the cerebellum. The absence of specific binding was defined as the presence of the highest values of the Hypotime measure associated with the white matter regions of cerebellum. In the distribution of Θ'' values, we chose the region corresponding to the highest 8% of the values as the reference mask with the least regional heterogeneity and the highest blood flow because of the least specific binding. On visual inspection, the voxels included in the mask remained within the anatomic boundaries of the white matter of the cerebellum. Figure 1 presents the Θ'' map and the cerebellar mask.

^{11}C -WAY Uptake and Clearance from Regions

Figure 2 illustrates the average time–activity curves of the groups of young and elderly subjects in the hippocampus, insula, and cingulate gyrus bilaterally. In these regionally averaged records, the curves show that the latter part of the washout curves declines monoexponentially. In general, the level of radioactivity in the selected

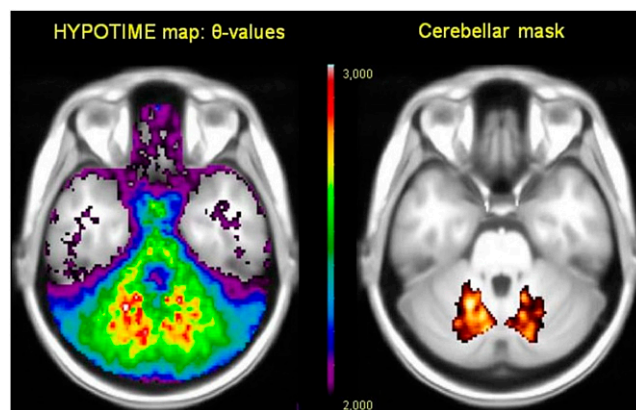


FIGURE 1. Θ'' map (left) and cerebellar mask (right).

regions was higher in the group of young subjects than in the elderly group.

Figure 3 shows the distribution of R_1 ratios based on frames 5–9 in 2,000 randomly selected voxels in each subject in the groups of young and elderly volunteers. The ratios R_1 were obtained from the peak values of the ^{11}C -WAY uptake images (plotted in the abscissa) versus ratios obtained from the images of the water distribution (plotted on the ordinate), as calculated according to Equation 7. The figure demonstrates the approximately linear relationship between the rapid and brief initial clearances of the 2 tracers from the circulation to the tissue. The relationship confirms the flow-limitation of the initial deposit of ^{11}C -WAY presumed in the present application.

BP_{ND} by Hypotime Method and MLSRTM

Figure 4 shows the average parametric maps of the BP_{ND} determined in the 7 young and 12 elderly volunteers by the Hypotime method and MLSRTM. The distribution of receptor binding showed the highest values in the hippocampus and insula, with values on the order of 3–4 obtained by the Hypotime method and on the order of 2–3 obtained by the MLSRTM. In the raphé nuclei, BP_{ND} averaged 2 and 1, respectively. The average values of the BP_{ND} in basal ganglia and cerebellum were negligible by both methods. BP_{ND} maps obtained by the Hypotime method demonstrated the clearest discrimination among regions. The average magnitudes of BP_{ND} , determined by parametric Hypotime and MLSRTM analyses in the 9 ROIs in the 2 groups, are listed in Table 1.

The same average magnitudes of BP_{ND} are shown in Figure 5 as histograms of the distribution of BP_{ND} in the young and elderly for the Hypotime method and MLSRTM. By the Hypotime method, the regional BP_{ND} values in the medial temporal regions were greater in the young than in the elderly subjects, but age-related differences in other regions were smaller. The MLSRTM did not reveal differences of BP_{ND} between the 2 age groups. The linear

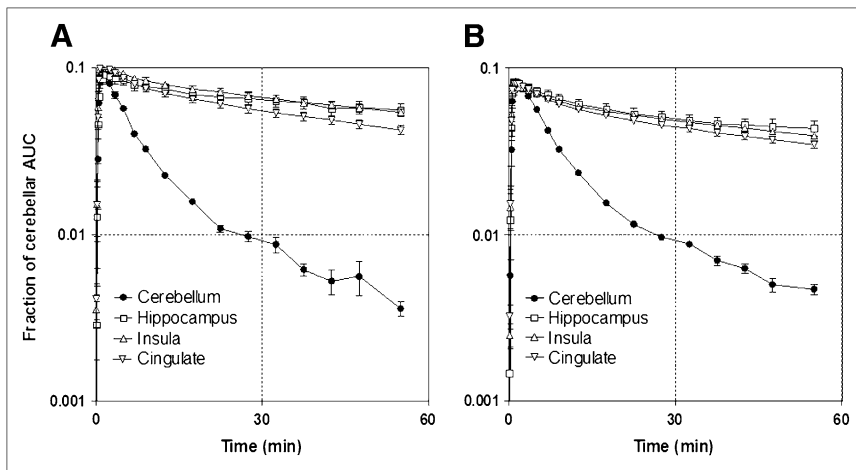


FIGURE 2. Time-activity curves from hippocampus, insula, and cingulate in young (A) and elderly (B) subjects. Abscissa, time (min); ordinate, log activity as fraction of average area under the curves of activity in cerebellum. AUC = area under curve.

correlation between the distributions of cortical BP_{ND} values by the 2 methods is shown in Figure 6.

DISCUSSION

The serotonin $5HT_{1A}$ receptor is of interest in studies of development, plasticity, and memory processes in the human brain (25–27), but the quantification of these receptors has been fraught with difficulty from the first publication of maps of BP_{ND} with the radioligand ^{11}C -WAY. In the present article, we argue that an appropriate method of analysis of ^{11}C -WAY binding must take the rapid disappearance of the radioligand ^{11}C -WAY from the circulation into account. We tested the results of the Hypotime method that uses the specific washout rates from different brain regions to estimate the magnitude of the volumes of distribution that delay the washout. The computationally efficient and accurate method involves no regression, and we found that reliable BP_{ND} can be obtained. The distribution of receptor BP_{ND} obtained with Hypotime in different brain regions is clearly consistent with previous results of autoradiography published by Hall et al. (17) and summarized for selected regions in Figure 7.

The main feature of the method is the calculation of BP_{ND} from washout rates corrected for different blood flow

rates on the basis of initial deposit of tracer. The initial deposit is flow-limited as shown in Figure 3, which shows that more than 60% of all initial deposit ratios (R_1) reside on a line of identity between the ratios of the radioligand and water as a flow tracer. Both the basic Hypotime measure (Θ'') and resulting BP_{ND} are model-independent as determined directly by calculation rather than by regression to a model-derived formula. This means that the BP_{ND} values obtained by parametric and ROI-based analyses do not diverge significantly as they tend to do when regression is involved.

The question is whether the results differ significantly from those of other methods, and also whether the variability of the BP_{ND} assessed in different subjects by different researchers changes significantly when the Hypotime method is used in place of more conventional methods. A potential concern in receptor mapping is the test-retest variability of the results. The differences in BP_{ND} values between age groups obtained by different kinetic models should be weighed against the reproducibility in previous receptor studies with ^{11}C -WAY. We found the variability to be in the range of 2%–15%, excluding the raphè (8,11), which is consistent with test-retest values in receptor studies of ^{11}C -labeled 3-amino-4-(2-dimethylaminomethyl-

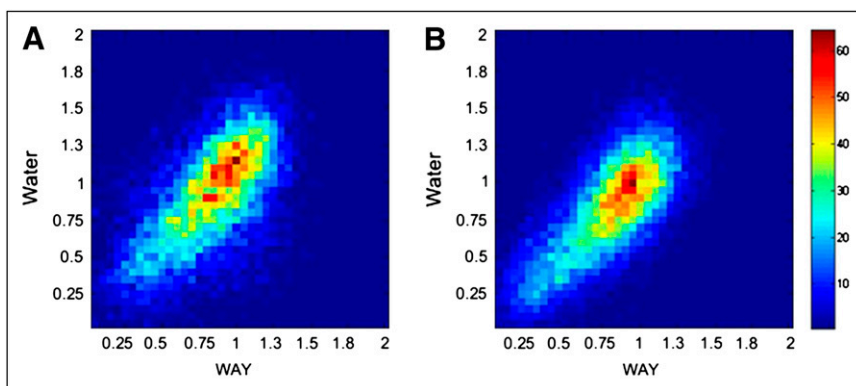


FIGURE 3. Accumulated radioactivity of water as index of cerebral blood flow, relative to cerebellum, vs. peak accumulation of ^{11}C -WAY, relative to cerebellum, in randomly selected voxels in groups of young (A) and elderly (B) subjects. Abscissae are R_1 ratios determined from ^{11}C -WAY; ordinates are R_1 ratios determined from water.

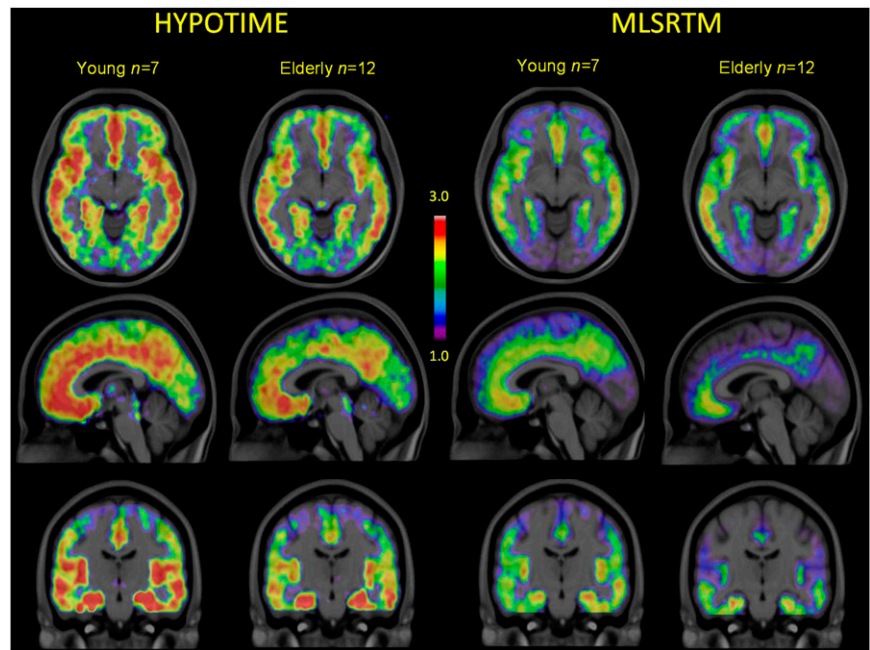


FIGURE 4. Parametric maps of BP_{ND} of radioligand ^{11}C -WAY in selected sections of brain tissue determined by 2 different methods, Hypotime and MLSRTM. Hypotime maps are shown to left, with columns with young and elderly subjects. MLSRTM maps are shown to right, with columns with young and elderly subjects.

phenylsulfanyl)-benzotrile, ^{18}F -2'-methoxyphenyl-(*N*-2'-pyridinyl)-*p*- ^{18}F -fluoro-benzamidoethylpiperazine, and ^{18}F -altanserin.

We compared the results of the Hypotime method with the results of other methods using a reference region. In a previous study, we compared the results of the MLSRTM with other methods used in current research (9), and in this study we compared Hypotime with the MLSRTM. With Hypotime, the highest values were found in the hippocampus and insula, whereas with the MLSRTM, no significant differences were observed among the regional values. The BP_{ND} maps obtained by Hypotime are consistent with the findings by autoradiography of receptor density in slices of brain obtained postmortem that show regionally differentiated binding, but this distribution is

not matched by the in vivo receptor map prepared with the MLSRTM from the same PET images of the radioligand uptake.

The Hypotime method demonstrated only subtle differences in the BP_{ND} from 30 to 55 min of the scan time as shown in Figure 8 of time-stability analysis based on washout in the group of young subjects, which indicates that a 60-min scan time is sufficient for the quantification of BP_{ND} using the radioligand ^{11}C -WAY.

The Hypotime method was useful also for the delineation of a proper reference region devoid of $5HT_{1A}$ receptors. It is possible that several kinds of ROIs could be defined by means of the functional Θ'' values rather than by comparatively crude anatomic boundaries, especially in structures with a heterogeneously distributed density

TABLE 1. Average Magnitudes of BP_{ND} , Determined by Parametric Hypotime and MLSRTM Analyses

Region	Hemisphere	Hypotime		MLSRTM	
		Young	Elderly	Young	Elderly
Hippocampus	Left	3.1 ± 0.5	2.6 ± 0.6	2.0 ± 0.4	1.8 ± 0.4
	Right	3.1 ± 0.6	2.6 ± 0.6	2.0 ± 0.3	1.9 ± 0.5
Cingulate gyrus	Left	2.4 ± 0.5	2.1 ± 0.4	1.9 ± 0.3	1.7 ± 0.3
	Right	2.3 ± 0.5	2.1 ± 0.4	1.7 ± 0.4	1.8 ± 0.3
Insula	Left	3.0 ± 0.4	2.4 ± 0.4	2.1 ± 0.3	2.0 ± 0.3
	Right	2.9 ± 0.5	2.4 ± 0.5	2.1 ± 0.3	2.0 ± 0.4
Medial prefrontal cortex	Left	2.7 ± 0.3	2.4 ± 0.3	1.9 ± 0.3	1.9 ± 0.3
	Right	2.7 ± 0.4	2.4 ± 0.3	1.9 ± 0.3	2.1 ± 0.3
Raphe		2.0 ± 0.4	1.7 ± 0.3	0.8 ± 0.2	1.0 ± 0.2
Global mean ± SD		2.7 ± 0.5	2.3 ± 0.3	1.8 ± 0.3	1.8 ± 0.3

Data are mean ± SD.

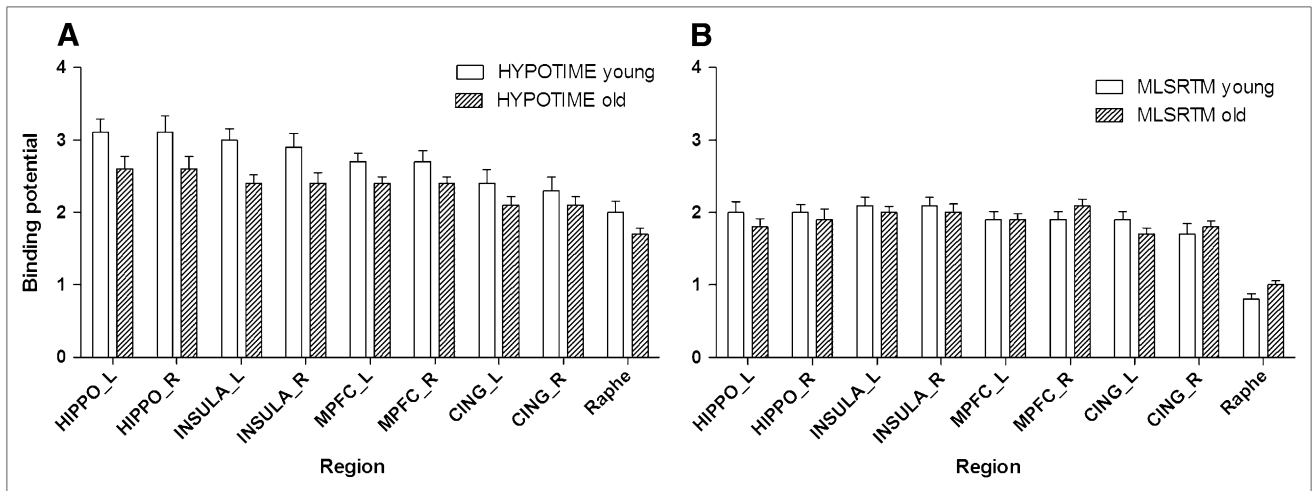


FIGURE 5. Histograms of distribution of BP_{ND} in selected ROIs in groups of young and elderly adults measured by Hypotime method (A) and MLSRTM (B).

of receptors in the layers of cortices such as the hippocampus.

The Hypotime method demonstrated a correlation with age in the regions of the highest BP_{ND} , such as the hippocampus and insula. In general, however, an age effect must be regarded with caution because of the multiple interpretations of BP_{ND} and the unknown relative contributions from changes in affinity, concentration of endogenous ligand, and receptor density.

CONCLUSION

For tracers such as ^{11}C -WAY used here, conventional reference region methods are subject to the variability associated with early disappearance of the radioligand from the circulation and the associated uncertain determination of late concentrations in the circulation. In contrast, the Hypotime method gives regionally specific values of binding to the serotonin $5HT_{1A}$ receptors, in the form of receptor availabilities. The method is simple and computationally convenient, because no regression is involved. The effect of age is seen most significantly only in the regions of the highest receptor availabilities.

ACKNOWLEDGMENTS

We thank the University of Aarhus, Denmark's National Science Foundation, and the Medical Research Council of Denmark for support of this study. This work was supported in part by a fellowship from the Clinical Institute of the University of Aarhus, a Center of Excellence grant from Denmark's National Science Foundation to CFIN, and operating grants from the Medical Research Council of Denmark.

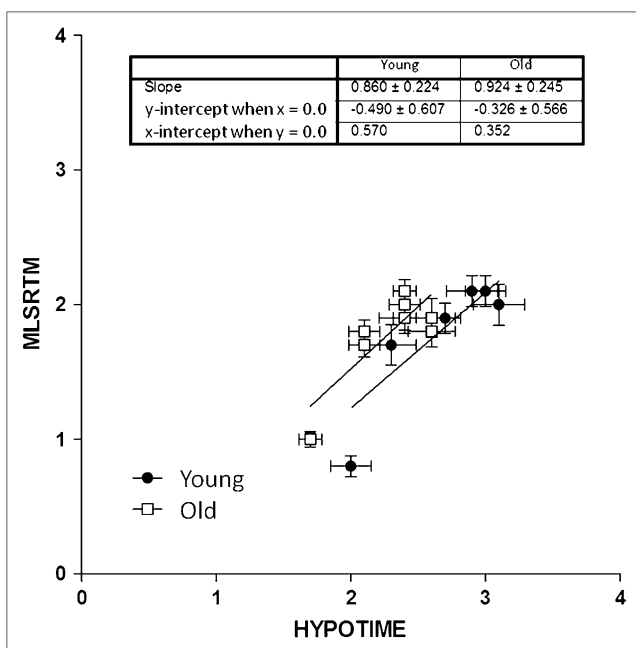


FIGURE 6. Scatterplot of BP_{ND} values of 9 ROIs obtained by Hypotime method and MLSRTM based on 12 elderly and 7 young healthy subjects.

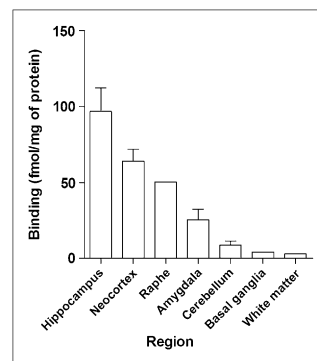


FIGURE 7. Histogram of averaged autoradiographic locations of $5HT_{1A}$ receptors in postmortem human brain obtained with 3H -WAY-100635 (17).

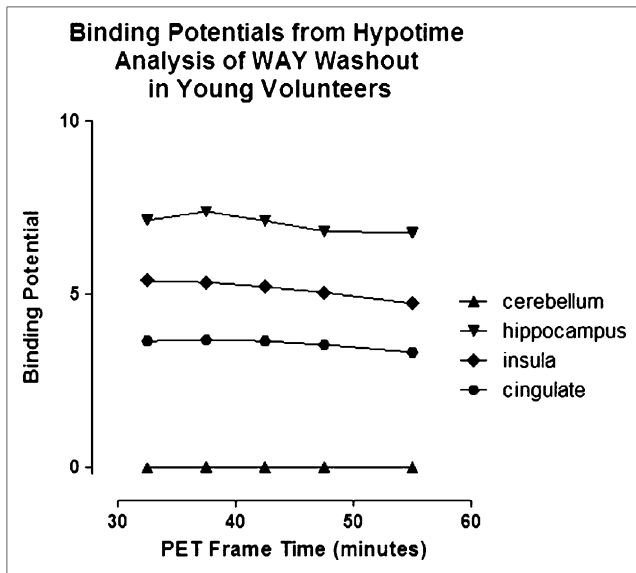


FIGURE 8. Time-stability analysis based on washout in group of young subjects.

REFERENCES

- Sargent PA, Kjaer KH, Bench CJ, et al. Brain serotonin_{1A} receptor binding measured by positron emission tomography with [¹¹C]WAY-100635: effects of depression and antidepressant treatment. *Arch Gen Psychiatry*. 2000;57:174–180.
- Tiihonen J, Keski-Rahkonen A, Lopponen M, et al. Brain serotonin_{1A} receptor binding in bulimia nervosa. *Biol Psychiatry*. 2004;55:871–873.
- Turner MR, Rabiner EA, Hammers A, et al. [¹¹C]-WAY100635 PET demonstrates marked 5-HT_{1A} receptor changes in sporadic ALS. *Brain*. 2005;128:896–905.
- Tauscher J, Kapur S, Verhoeff NP, et al. Brain serotonin 5-HT_{1A} receptor binding in schizophrenia measured by positron emission tomography and [¹¹C]WAY-100635. *Arch Gen Psychiatry*. 2002;59:514–520.
- Doder M, Rabiner EA, Turjanski N, Lees AJ, Brooks DJ. Tremor in Parkinson's disease and serotonergic dysfunction: an [¹¹C]-WAY 100635 PET study. *Neurology*. 2003;60:601–605.
- Savic I, Lindstrom P, Gulyas B, Halldin C, Andree B, Farde L. Limbic reductions of 5-HT_{1A} receptor binding in human temporal lobe epilepsy. *Neurology*. 2004;62:1343–1351.
- Rabiner EA, Messa C, Sargent PA, et al. A database of [¹¹C]WAY-100635 binding to 5-HT_{1A} receptors in normal male volunteers: normative data and relationship to methodological, demographic, physiological, and behavioral variables. *Neuroimage*. 2002;15:620–632.
- Hirvonen J, Kajander J, Allonen T, Oikonen V, Nagren K, Hietala J. Measurement of serotonin 5-HT_{1A} receptor binding using positron emission tomography and [¹¹C]WAY-100635: considerations on the validity of cerebellum as a reference region. *J Cereb Blood Flow Metab*. 2007;27:185–195.

- Moller M, Jakobsen S, Gjedde A. Parametric and regional maps of free serotonin 5HT_{1A} receptor sites in human brain as function of age in healthy humans. *Neuropsychopharmacology*. 2007;32:1707–1714.
- Parsey RV, Oquendo MA, Simpson NR, et al. Effects of sex, age, and aggressive traits in man on brain serotonin 5-HT_{1A} receptor binding potential measured by PET using [¹¹C]WAY-100635. *Brain Res*. 2002;954:173–182.
- Tauscher J, Verhoeff NP, Christensen BK, et al. Serotonin 5-HT_{1A} receptor binding potential declines with age as measured by [¹¹C]WAY-100635 and PET. *Neuropsychopharmacology*. 2001;24:522–530.
- Bhagwagar Z, Rabiner EA, Sargent PA, Grasby PM, Cowen PJ. Persistent reduction in brain serotonin_{1A} receptor binding in recovered depressed men measured by positron emission tomography with [¹¹C]WAY-100635. *Mol Psychiatry*. 2004;9:386–392.
- Hume S, Hirani E, Opacka-Juffry J, et al. Effect of 5-HT on binding of [¹¹C]WAY 100635 to 5-HT_{1A} receptors in rat brain, assessed using in vivo microdialysis and PET after fenfluramine. *Synapse*. 2001;41:150–159.
- Maeda J, Suhara T, Ogawa M, et al. In vivo binding properties of [¹¹C]WAY-100635: effect of endogenous serotonin. *Synapse*. 2001;40:122–129.
- Gunn RN, Sargent PA, Bench CJ, et al. Tracer kinetic modeling of the 5-HT_{1A} receptor ligand [¹¹C]WAY-100635 for PET. *Neuroimage*. 1998;8:426–440.
- Osman S, Lundkvist C, Pike VW, et al. Characterisation of the appearance of radioactive metabolites in monkey and human plasma from the 5-HT_{1A} receptor radioligand, [¹¹C]WAY-100635: explanation of high signal contrast in PET and an aid to biomathematical modelling. *Nucl Med Biol*. 1998;25:215–223.
- Hall H, Lundkvist C, Halldin C, et al. Autoradiographic localization of 5-HT_{1A} receptors in the post-mortem human brain using [³H]WAY-100635 and [¹¹C]WAY-100635. *Brain Res*. 1997;745:96–108.
- Parsey RV, Arango V, Olvet DM, Oquendo MA, Van Heertum RL, John MJ. Regional heterogeneity of 5-HT_{1A} receptors in human cerebellum as assessed by positron emission tomography. *J Cereb Blood Flow Metab*. 2005;25:785–793.
- Zhou Y, Endres CJ, Brasic JR, Huang SC, Wong DF. Linear regression with spatial constraint to generate parametric images of ligand-receptor dynamic PET studies with a simplified reference tissue model. *Neuroimage*. 2003;18:975–989.
- American Psychiatric Association. *Diagnostic and Statistical Manual of Mental Disorders. DSM-IV*. 4th ed. Washington, DC: American Psychiatric Association; 1994.
- McCarron JA, Turton DR, Pike VW, Poole KG. Remotely-controlled production of the 5HT_{1A} receptor radioligand, [¹¹C]WAY-100635, via ¹¹C-carboxylation of an immobilized Grignard reagent. *J Labelled Comp Radiochem*. 1996;38:941–953.
- Collins DL, Neelin P, Peters TM, Evans AC. Automatic 3D intersubject registration of MR volumetric data in standardized Talairach space. *J Comput Assist Tomogr*. 1994;18:192–205.
- Gjedde A. Modelling metabolite and tracer kinetics. In: Feinendegen LE, Shreeve WW, Eckelman WC, Bahk Y-W, Wagner HN Jr, eds. *Molecular Nuclear Medicine*. Berlin, Germany: Springer-Verlag; 2003:121–169.
- Gompertz B. On the nature of the function expressive of the law of human mortality, and on a new mode of determining the value of life contingencies. *Philos Trans R Soc Lond*. 1825;115:513–583.
- Whitaker-Azmitia PM. Serotonin and brain development: role in human developmental diseases. *Brain Res Bull*. 2001;56:479–485.
- Santarelli L, Saxe M, Gross C, et al. Requirement of hippocampal neurogenesis for the behavioral effects of antidepressants. *Science*. 2003;301:805–809.
- Ridley RM, Harder JA, Baker HF. Neurochemical modulation of the hippocampus in learning, remembering and forgetting in primates. *Neurodegeneration*. 1996;5:467–471.